Available online at www.sciencedirect.com
ScienceDirect
Journal of Power Sources 166 (2007) 47–52
JOURNAL OF POWER SOURCES
www.elsevier.com/locate/jpowsour

Short communication

Synthesis and properties of Y-doped $SrTiO_3$ as an anode material for SOFCs

Xue Li [a], Hailei Zhao [a,*], Wei Shen [a], Feng Gao [a], Xianliang Huang [a], Yue Li [a], Zhiming Zhu [b]

[a] *Department of Inorganic Nonmetallic Materials, University of Science and Technology Beijing, Beijing 100083, PR China*
[b] *Department of Mechanical Engineering, Tsinghua University, Beijing 100084, PR China*

Received 7 December 2006; received in revised form 28 December 2006; accepted 2 January 2007
Available online 16 January 2007

Abstract

Y-doped $SrTiO_3$ was synthesized via solid-state reaction. The effects of Y-doping on the sinterability and the electrical conductivity of $Y_xSr_{1-x}TiO_3$ were investigated. Y-doping can increase the sintering activity and the electrical conductivity of $SrTiO_3$ when yttrium amount is less than 0.09 in $Y_xSr_{1-x}TiO_3$. Excessive yttrium will cause the generation of an insulating phase $Y_2Ti_2O_7$, which impedes the densification process and decreases the electrical conductivity of $Y_xSr_{1-x}TiO_3$ material. With the increased temperature, the electrical conductivity of Y-doped $SrTiO_3$ increases first and then decreases gradually, showing a mixed conduction behavior of semi-conductors and metals. The optimized $Y_{0.09}Sr_{0.91}TiO_3$ possesses an electrical conductivity on the order of 32.5–195.8 S cm^{-1} in the temperature range of 25–1000 °C and being 73.7 S cm^{-1} at 800 °C in forming gas. The thermal cycling in air does not remarkably affect the electrical conductivity and the conduction behavior of $Y_{0.09}Sr_{0.91}TiO_3$ at high temperatures. $Y_{0.09}Sr_{0.91}TiO_3$ displays a relatively stable electrical conductivity at different oxygen partial pressures and excellent chemical compatibility with YSZ at temperatures lower than 1300 °C.

Keywords: Solid oxide fuel cell; Anode; Y-doped $SrTiO_3$; Electrical conductivity

1. Introduction

The solid oxide fuel cell (SOFC) as an all-ceramic power generation system has attracted more attention due to its many advantages over conventional power generation systems in terms of high efficiency, fuel adaptability and low pollution [1,2]. In SOFC systems, YSZ (yttria-stabilized zirconia), $La_{1-x}Sr_xMnO_3$ (strontium-doped lanthanum manganite), Ni/YSZ cermet and $La_{1-x}Ca_xCrO_3$ (calcium-doped lanthanum chromite) or commercial ferritic stainless steels are respectively used as electrolyte, cathode, anode and interconnect materials at present [3–5]. The most commonly used Ni/YSZ anode material possesses high electronic and ionic conductivities as well as sufficient catalytic activity towards the oxidation of hydrogen occurring at anode side. However, it shows some disadvantages, such as low tolerance to sulfur and carbon deposition when using hydrocarbon as fuels, and poor redox cyclability and volume stability due to the oxidation of Ni [6]. Therefore, new anode materials are in demands for further development of SOFCs.

Perovskites are good candidates for anode materials because they are known to possess properties such as high electronic conductivity, high oxide ion conductivity and good catalytic activity. Strontium titanate, $SrTiO_3$, with perovskite structure, is one of the promising anode materials for SOFCs. It shows strong carbon deposition resistance and good structural stability compared with Ni/YSZ cermet. However, its low electrical conductivity and poor catalytic activity towards the oxidation of fuels prevent $SrTiO_3$ as a practical anode for SOFCs. Doping with aliovalent elements on A or B site of $SrTiO_3$ is an effective approach to increase the electrical conductivity, improve the catalytic activity and control the thermal expansion coefficient of $SrTiO_3$ materials. Doping donors such as La^{3+} on the Sr^{2+} site and Nb^{5+} on the Ti^{4+} site converts $SrTiO_3$ into a highly semiconducting n-type material [7,8], while a p-type material was achieved by doping acceptors such as Fe^{3+} and Al^{3+} on the Ti^{4+} site [9,10]. Hui and Petric [11,12] and Obara et al. [13] have studied the electrical properties of $Y_xSr_{1-1.5x}TiO_3$, where strontium vacancies are supposed to be created in Y-doped $SrTiO_3$ accord-

* Corresponding author. Tel.: +86 10 62334863; fax: +86 10 62332570.
E-mail address: hlzhao@mater.ustb.edu.cn (H. Zhao).

0378-7753/$ – see front matter © 2007 Elsevier B.V. All rights reserved.
doi:10.1016/j.jpowsour.2007.01.008

ing to the chemical formula. In this study, we investigated the electrical conduction behavior of Y-doped $SrTiO_3$ in the form of $Y_xSr_{1-x}TiO_3$, where a certain amount of Ti^{3+} is supposed to be produced as charge compensation and accordingly electron defects should be formed in $Y_xSr_{1-x}TiO_3$. The effects of Y amount on the properties of $Y_xSr_{1-x}TiO_3$ in terms of sinterability and electrical conductivity as a function of temperature and oxygen partial pressure were investigated. The chemical compatibility of $Y_xSr_{1-x}TiO_3$ with YSZ electrolyte was also examined.

2. Experimental

Yttrium-doped and undoped $SrTiO_3$ powers ($Y_xSr_{1-x}TiO_3$, $x = 0$, 0.02, 0.08, 0.09 and 0.12) were synthesized at 1300 °C for 10 h in forming gas (5 vol.% hydrogen in argon) from high pure TiO_2, Y_2O_3 and $SrCO_3$ by conventional solid-state reaction after ball milling for 6 h. The heating and cooling rates were 4 °C min^{-1}. The so-obtained powders were pressed into bars (40 mm × 7 mm × 3 mm) by uniaxial pressing (ca. 115 MPa) without a binder and then sintered at 1500 °C for 10 h in forming gas to prepare dense samples. The phase composition was determined by X-ray diffraction (XRD, Rigaku D/max-A X-ray diffractometer) using Cu Kα radiation. A Cambridge S250-MK2 scanning electron microscope (SEM) was employed to observe the microstructure of the sintered samples. The density of sintered samples was estimated by the dimensions and the weights of the samples.

The electrical conductivity of all samples was measured in forming gas by the standard four-terminal dc method [14–16] in the temperature range of 25–1000 °C, with a heating rate of 4 °C min^{-1}. The four-terminal method is suitable to materials having moderate to high conductivities. With this method the effect of non-ohmic contacts or barrier layers can be overcome. Sintered bars for conductivity measurements were wrapped with four wires which were held in place by small notches cut on the sample surfaces. All measurements were taken after holding at each temperature to equilibrate for at least 15 min and no significant change in electrical conductivity was observed. To evaluate the thermal stability of Y-doped $SrTiO_3$, the sample was cooled in air with powered off furnace after electrical conductivity measurement at 1000 °C in forming gas and then heated up again in forming gas to different temperatures to determine the electrical conductivity changes. The dependence of conductivities on oxygen partial pressure (P_{O_2}) was also investigated under P_{O_2} from 10^{-19} to 10^{-14} atm. The oxygen partial pressure was adjusted by changing the mixing ratio of argon, hydrogen and water vapor. The water vapor partial pressure of the mixture gases was generated by flowing forming gas through the water vapor saturator, which was installed outside the furnace. The temperature of the water vapor saturator was changed from room temperature to 100 °C. Flow rate of these mixture gases was 20 cm^3 min^{-1} [17,18]. To examine the compatibility of $Y_xSr_{1-x}TiO_3$ with YSZ, the 1500 °C-fired Y-doped $SrTiO_3$ was mixed with YSZ in the weight ratio of 1:1, followed by uniaxial pressing and sintering at different temperatures.

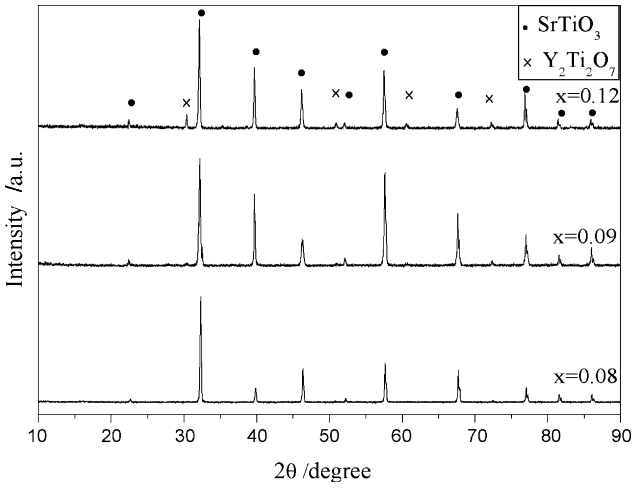

Fig. 1. XRD patterns of $Y_xSr_{1-x}TiO_3$ after sintered at 1500 °C.

3. Results and discussion

3.1. Phase and microstructure development

The phase composition of dense samples $Y_xSr_{1-x}TiO_3$ after sintered at 1500 °C for 10 h was identified with XRD. The results are shown in Fig. 1. The samples with $x \leq 0.08$ shows a single cubic perovskite structure and no impurity peaks are detected, while for the one with $x = 0.09$, a trace amount of impurity phase is observed. When $x = 0.12$, an obvious second phase $Y_2Ti_2O_7$ presents. Thus it is reasonable to state that the doping limit of Y in $SrTiO_3$ at 1500 °C is less than 9 mol%. The relative density of dense $Y_xSr_{1-x}TiO_3$ samples as a function of doping amount is presented in Fig. 2. It increases before $x = 0.08$ and decreases after that with increasing Y-doping amount, indicating that Y-doping that can form single phase solid solution with $SrTiO_3$ will lead to the high sinterability of $SrTiO_3$ materials, while excessive Y-doping that will cause the appearance of impurity $Y_2Ti_2O_7$ will impede the densification process of $SrTiO_3$ materials.

The SEM micrographs of fracture surfaces of dense $Y_xSr_{1-x}TiO_3$ ($x = 0.02$, 0.08, 0.09) samples are illustrated in

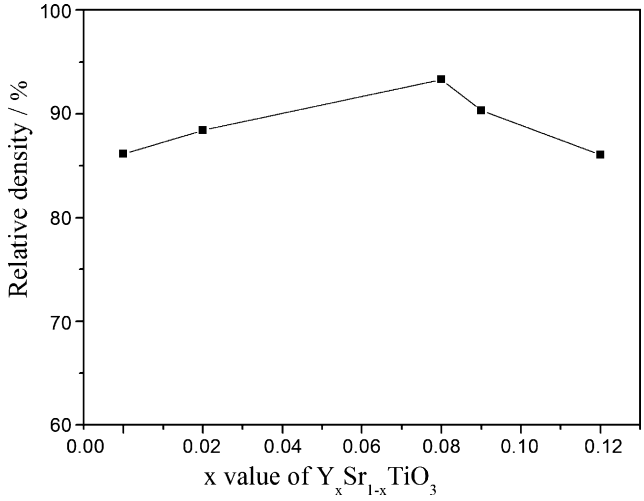

Fig. 2. Relation between relative density and x value in $Y_xSr_{1-x}TiO_3$.

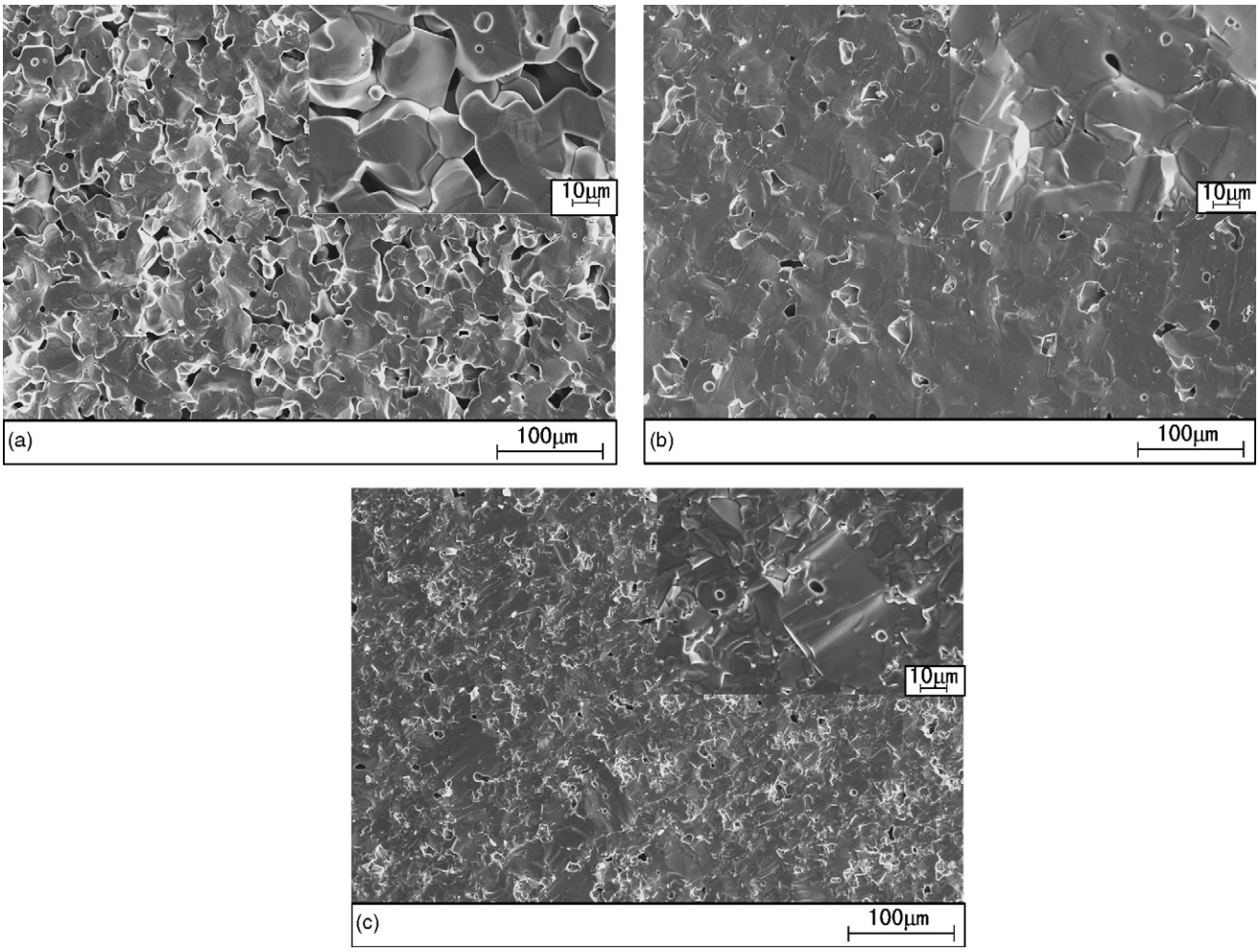

Fig. 3. SEM micrographs of fracture surfaces of $Y_xSr_{1-x}TiO_3$ sintered at 1500 °C for 10 h, $x = 0.02$ (a); $x = 0.08$ (b); $x = 0.09$ (c).

Fig. 3. The sample with $x = 0.02$ shows a loose microstructure with a large amount of grain-boundary pores (Fig. 3a). With the increasing Y-doping amount, the porosity decreases. A quiet amount of grain-boundaries have been formed in sample with $x = 0.08$, as shown in Fig. 3b, indicating that the Y-doping can promote the densification process of $SrTiO_3$ material. However, excessive yttrium ($x = 0.09$) results in a small grain size and a high porosity, as displayed in Fig. 3c.

A reasonable explanation could be that the Y donor-doping will result in the higher activity of powders, which is favorable to the sintering of bulks. Grain growth in $SrTiO_3$ has been reported to be highly sensitive to donor-doping [19–21]. Grain growth may become pronounced with Y-doping during sintering process, however, the trace impurity existing in the sample with $x = 0.09$ may impede the mass transportation and the sintering process, thus leading to a high porosity and a low density compared to the sample with $x = 0.08$. This is consistent with the results shown in Fig. 2.

3.2. Electrical characteristics of Y-doped strontium titanate

The electrical conductivity of samples $Y_xSr_{1-x}TiO_3$ ($x = 0$, 0.02, 0.08, 0.09, 0.12) was measured in forming gas in the temperature range of 25–1000 °C. It increases with Y-doping amount when $x \leq 0.09$, while it tends to decrease with doping amount when $x > 0.09$ (Fig. 4). This regularity can be explained by defect chemistry. Ti^{3+} ions will be produced in $Y_xSr_{1-x}TiO_3$

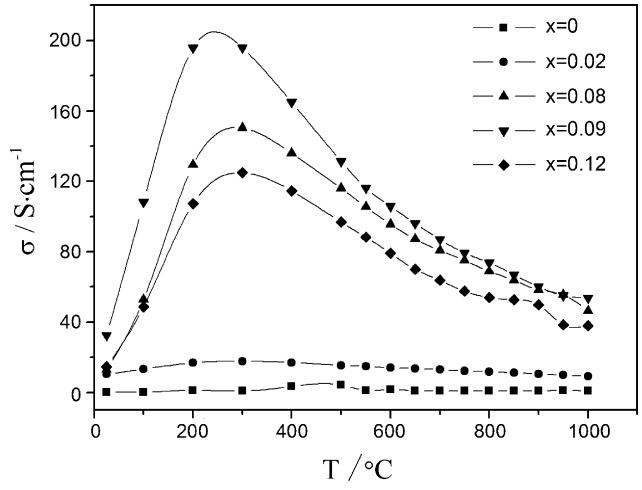

Fig. 4. Temperature dependence of electrical conductivity of $Y_xSr_{1-x}TiO_3$ measured in forming gas at different temperatures.

for the electrovalent compensation in reducing condition. So the defects produced in Y donor-doping $SrTiO_3$ can be expressed as

$$Y_2O_3 \xrightarrow{SrTiO_3} 2Y_{Sr}^{\bullet} + 2e' + 3O_o^x \quad (1)$$

Oxygen vacancies also may occur at low oxygen partial pressure, which can be described as

$$O_o^x \rightarrow V_O^{\bullet\bullet} + 2e' + \tfrac{1}{2}O_2 \quad (2)$$

The produced electrons will be localized in titanium sites to form Ti^{3+}.

In this case, electrons bonded on Ti ions and oxygen vacancies are the main defects. Due to the low mobility of oxygen vacancies compared with electrons, oxygen vacancies will make little contribution to the conductivity of Y-doped $SrTiO_3$ material. As a result, the conductivity of Y-doped $SrTiO_3$ in reducing condition mostly depends on the concentration of localized electrons. The concentration of localized electrons at a constant oxygen partial pressure for a relatively large amount of dopants can be expressed as

$$n \approx [D^{\bullet}] \quad (3)$$

where D is the donor.

The number of compensated Ti^{3+} with localized electrons increases with increasing yttrium incorporated in $SrTiO_3$ and the concentration of oxygen vacancies depends on the oxygen partial pressure. Therefore, the electrical conductivity of $Y_xSr_{1-x}TiO_3$ increases with increasing Y amount when x value is not more than 9 mol%. While excessive dopant may cause the electrical conductivity decreases because of the formation of insulating impurity ($Y_2Ti_2O_7$) with the exception of $Y_{0.09}Sr_{0.91}TiO_3$, whose conductivity is even higher than $Y_{0.08}Sr_{0.92}TiO_3$. It is very possible that the doping limit of Y in $SrTiO_3$ is in the range of 8–9 mol% at 1500 °C, according to the XRD results shown in Fig. 1. For doping amount of 9 mol%, the additional 1 mol% Y in comparison with 8 mol% yttrium-doped $SrTiO_3$ will produce a certain amount of Ti^{3+} as charge compensation and a trace of $Y_2Ti_2O_7$ due to the solid solution limitation. The former, compared to the latter, may play a predominant role in charge transportation and thus resulting in a higher electrical conductivity. The optimized $Y_{0.09}Sr_{0.91}TiO_3$ exhibits an electrical conductivity on the order of 32.5–195.8 S cm^{-1} and being 73.7 S cm^{-1} at 800 °C. The electrical conductivity of $SrTiO_3$ is remarkably enhanced by Y-doping.

The electrical conductivity of Y-doped $SrTiO_3$ (Fig. 4) shows a mixed conduction behavior with increasing temperature. At low temperature (between room temperature and 300 °C), the electrical conductivity of $Y_xSr_{1-x}TiO_3$ samples increases remarkably with increasing temperature, indicating a polaron-type conduction mechanism. The localized electrons at Ti site will hop between Ti^{3+} and Ti^{4+} via bridging oxygen atoms, and thus produce electronic conductivity. With the temperature increasing, the electron hopping is activated and becomes much easier, thus leading to an increased electronic conductivity. The high concentration of Ti^{3+} caused by Y-doping will enhance the hopping process of electrons, and consequently result in an improved conductivity with Y-doping amount. Exceeding a critical temperature (ca. 300 °C), the electrical conduction of Y-doped $SrTiO_3$ transforms from semi-conducting to metallic behavior, the localized electrons are delocalized and become free electrons. As a result, the electrical conductivities of all the Y-doped $SrTiO_3$ samples decrease with increasing temperature due to the decreasing mobility of the electrons. This suggests that electronic conduction should be the predominant electrical conduction mechanism in the investigated Y-doped $SrTiO_3$ samples.

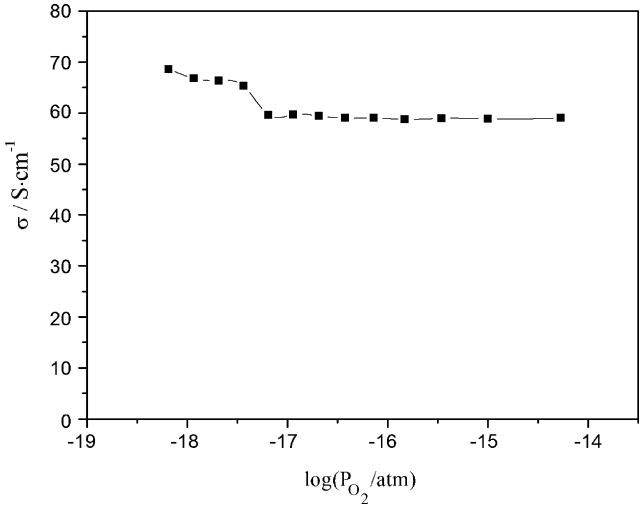

Fig. 5. Effect of oxygen partial pressure (P_{O_2}) on electrical conductivity of $Y_{0.09}Sr_{0.91}TiO_3$ at 800 °C.

In fuel cell systems, anode is the channel of fuel with a reducing atmosphere, and on the other hand, it is also the place for reaction with a faint oxidizing atmosphere. Therefore, it is necessary for anode material to have good stability in wide oxygen partial pressure range. As given in Fig. 5, with the decreasing oxygen partial pressure the electrical conductivity of $Y_{0.09}Sr_{0.91}TiO_3$ keeps unchanged in the oxygen partial pressure range of 10^{-14} to 10^{-17} atm, while shows a slight increase when the oxygen partial pressure is lower than 10^{-17} atm. This indicates the relatively good structural stability of Y-doped $SrTiO_3$ under different reducing conditions. The slight increase in conductivity with decreased oxygen pressure comes from the release of lattice oxygen into the surrounding atmosphere, which will result in the increase of both oxygen vacancies and electrons, as shown in Eq. (2).

To be a useful anode material for fuel cells, the thermal stability and the compatibility with electrolyte are of great importance. In this work, the thermal stability of $Y_{0.09}Sr_{0.91}TiO_3$ was evaluated by comparing its electrical conductivity in forming gas before and after thermal cycling in air. Fig. 6 reveals that the electrical conductivity of cycled $Y_{0.09}Sr_{0.91}TiO_3$ is much lower than uncycled sample before 300 °C. This is considered to be resulted from the incorporation of oxygen vacancies with surrounding oxygen in the course of cooling in air as a reverse process of Eq. (2), which will lead to the decrease of both oxygen vacancies and electrons in $Y_{0.09}Sr_{0.91}TiO_3$. After 300 °C, the electrical conductivity of cycled sample increases slightly upon temperature, probably due to the loss of lattice oxygen of

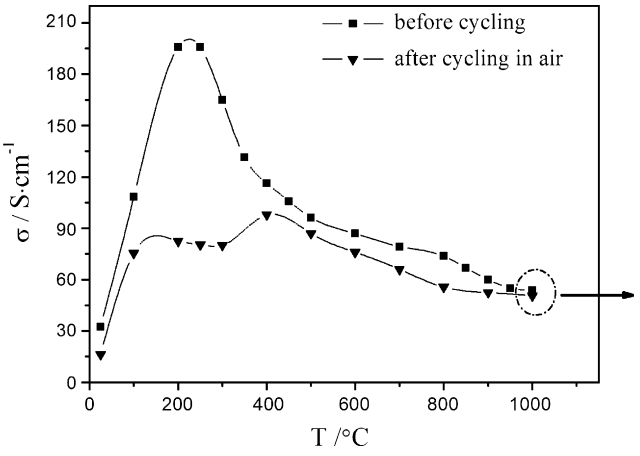

Fig. 6. Electrical conductivity of $Y_{0.09}Sr_{0.91}TiO_3$ in forming gas before and after thermal cycling in air.

$Y_{0.09}Sr_{0.91}TiO_3$ at high temperature and reducing atmosphere, which will result in the increase of oxygen vacancies and electrons simultaneously as shown in Eq. (2). Beyond 400 °C, the cycled sample show the similar conductivity value with sample before cycling, indicating that the structure of cycled sample has been recovered and reached a stable state. Compared with 53.66 S cm^{-1} of the uncycled sample, the cycled sample shows an electrical conductivity of 50.61 S cm^{-1} at 1000 °C and there was no decline after keeping at 1000 °C for 50 h, as shown in Fig. 7. It suggests that the thermal cycling in this experiment has little effect on the electrical conductivity of $Y_{0.09}Sr_{0.91}TiO_3$ at temperature higher than 400 °C.

In order to assess the chemical compatibility of $Y_{0.09}Sr_{0.91}TiO_3$ with YSZ, powder mixture of $Y_{0.09}Sr_{0.91}TiO_3$ and YSZ in the weight ratio of 1:1 were pressed into bars after milling for 6 h and then sintered at 1100, 1200 and 1300 °C for 10 h, respectively. The sintered samples of $Y_{0.09}Sr_{0.91}TiO_3$/YSZ were examined by XRD, and the results are shown in Fig. 8. No impurity peaks were detected except for that assignable to $SrTiO_3$ and YSZ, indicating that $Y_{0.09}Sr_{0.91}TiO_3$ material has a good chemical compatibility with YSZ below 1300 °C.

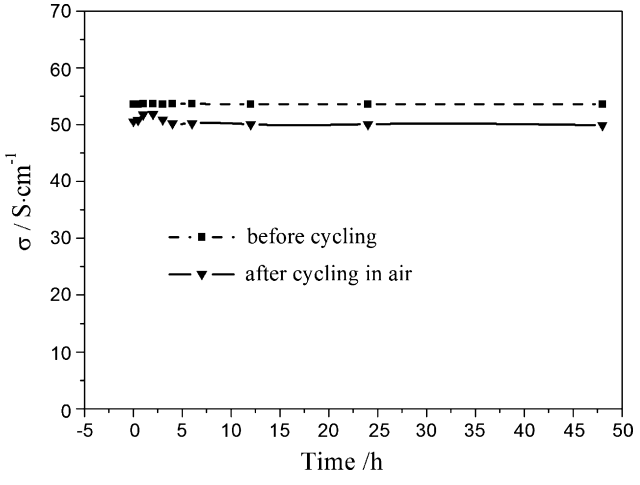

Fig. 7. Time dependence of electrical conductivity of $Y_{0.09}Sr_{0.91}TiO_3$ at 1000 °C in forming gas before and after thermal cycling in air.

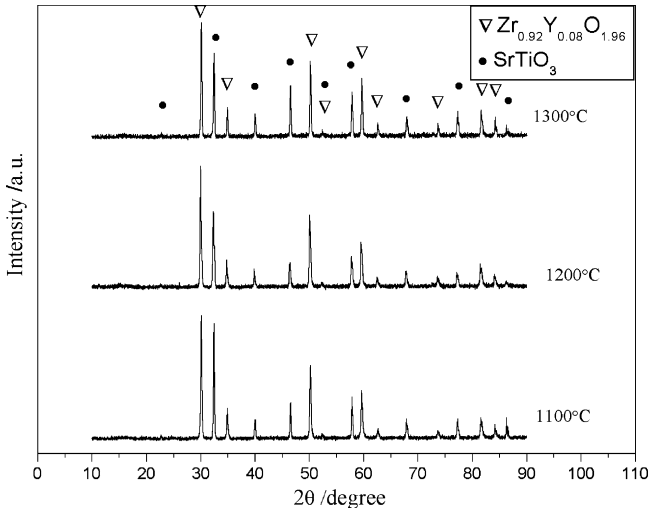

Fig. 8. XRD patterns for $Y_{0.09}Sr_{0.91}TiO_3$/YSZ powder mixtures sintered at 1100, 1200 and 1300 °C for 10 h respectively in forming gas. No new impurity peaks were detected.

4. Conclusions

The electrical conductivity of $SrTiO_3$ is remarkably enhanced by Y-doping. It increases with increasing Y amount when the doping amount is no more than 9 mol%. Excessive dopant may cause the electrical conductivity to decrease because of the formation of an insulating impurity ($Y_2Ti_2O_7$). With increased temperature, the electrical conductivity of Y-doped $SrTiO_3$ increases first and then decreases gradually, showing a mixed conduction behavior of semi-conductors and metals. The thermal cycling in air does not remarkably affect the electrical conductivity of $Y_{0.09}Sr_{0.91}TiO_3$ at high temperatures. $Y_{0.09}Sr_{0.91}TiO_3$ displays a relatively good structural stability at different oxygen partial pressures and excellent chemical compatibility with YSZ at temperatures lower than 1300 °C.

Acknowledgement

This work was supported by National Nature Science Foundation of China (No. 50672009).

References

[1] D. Masayuki, Solid State Ionics 152–153 (2002) 383–392.
[2] H.C. Yu, F. Zhao, A.V. Virkar, K.Z. Fung, J. Power Sources 152 (2005) 22–26.
[3] C. Brugnoni, U. Ducati, M. Scagliotti, Solid State Ionics 76 (1995) 177–182.
[4] J.P.P. Huijsmans, F.P.F. van Berkel, G.M. Christie, J. Power Sources 71 (1998) 107–110.
[5] Z. Yang, G. Xia, J.W. Stevenson, J. Power Sources 160 (2006) 1104–1110.
[6] S. Tao, T.S. John, Irvine, J. Solid State Chem. 165 (2002) 12–18.
[7] O.N. Tufte, P.W. Chapman, Phys. Rev. 155 (1967) 796–802.
[8] H.P.R. Frederikse, W.R. Hosler, Phys. Rev. 161 (1967) 822–827.
[9] D.P. Fagg, V.V. Kharton, A.V. Kovalevsky, A.P. Viskup, E.N. Naumovich, J.R. Frade, J. Euro. Ceram. Soc. 21 (2001) 1831–1835.
[10] M. Widerøe, W. Münch, Y. Larring, T. Norby, Solid State Ionics 154–155 (2002) 669–677.
[11] S.Q. Hui, A. Petric, J. Euro. Ceram. Soc. 22 (2002) 1673–1681.

[12] S.Q. Hui, A. Petric, J. Electrochem. Soc. 149 (2002) 1–10.
[13] H. Obara, A. Yamamoto, C.H. Lee, Jpn. J. Appl. Phys. 43 (2004) 540–542.
[14] H. Ikawa, K. Shima, T. Taniguchi, K. Urabe, O. Fukunaga, J. Mizusaki, Solid State Ionics 35 (1989) 217–222.
[15] Y. Suzuki, T. Takahashi, N. Nagae, Solid State Ionics 3–4 (1981) 483–487.
[16] X. Huang, H. Zhao, W. Shen, W. Qiu, W. Wu, J. Phys. Chem. Solids 67 (2006) 2609–2613.
[17] N. Kitamura, K. Amezawa, Y. Tomii, T. Hanada, N. Yamamoto, Solid State Ionics 176 (2005) 2875–2879.
[18] H. Kurokawa, K. Kawamura, T. Maruyama, Solid State Ionics 168 (2004) 13–21.
[19] I. Burn, S. Neirman, J. Mater. Sci. 17 (1982) 3510–3524.
[20] M.F. Yan, Mater. Sci. Eng. 48 (1981) 53–72.
[21] M. Kahn, J. Am. Ceram. Soc. 54 (1971) 452–454.